

Final Technical Report

NEHRP External Grant Award Number 06HQGR0108
Recovering Absolute Seismic Displacements Through the
Combined Use of 1Hz GPS and Strong Motion Accelerometers

Prof. Jennifer S. Haase
Dept. of Earth & Atmos. Sci., Purdue University
550 Stadium Mall Dr
West Lafayette, IN 47907-2051
765-494-1643; 765-496-1210; jhaase@purdue.edu
Original Project Term: January 2006 - December 2007

NEHRP Element(s): I National and regional earthquake hazards assessments

Key Words: strong ground motion, continuous GPS

Abstract

Measuring absolute ground displacement with 1 Hz GPS observations is important for distinguishing between coseismic and early postseismic deformation during earthquakes and for correcting some of the most troublesome errors in seismic records from near source ground motions. We have developed a method for combining seismic and 1 Hz GPS observations in order to retrieve highly accurate displacement records. The magnitude of the error estimates in the 1 Hz GPS estimates is 3 to 7 mm on the horizontal components. A displacement time history that is constrained by both the observed GPS and strong motion accelerometer data, and which properly accounts for the error sources in each type of observation, is useful for investigation of the slip history in an event.

Retrieving displacement from seismic acceleration records is often difficult because unknown small offsets in the acceleration time series will contaminate the doubly integrated record with large parabolic errors. Baseline corrections that are typically applied may create a reasonable looking record, however the static offset and lower frequency information is not known to be reliable. We use the additional information that is provided by 1 Hz GPS to reliably retrieve the absolute displacement and the amplitude of lower frequency velocity pulses in the presence of these effects.

We developed an inversion method to simultaneously solve for ground displacement using both data sets as input constraints that takes into account the presence of unknown offsets in the acceleration record and the relatively large uncertainties in the processed 1 Hz GPS data. This work impacts both earthquake dynamics research and earthquake hazard mitigation. The interpretation of observations of rapid aseismic slip on earthquake faults represents a new challenge in understanding earthquake processes. This work will contribute to earthquake hazard mitigation by providing a technique to the earthquake

engineering community for determining near-source time histories that are reliable at low frequencies. This is important for testing the dynamic response of large structures and base isolation systems for the new generation of “smart buildings”, where large displacement pulses affect the design limits of the structure.

Introduction

The use of near-field strong ground motion acceleration records for both understanding the seismic source and for improving the response of buildings to strong shaking is subject to the correct interpretation of doubly integrated records that may have serious errors. These errors are typically hidden within the strong shaking portion of an acceleration record, and are only visible once the record is integrated. The errors in the accelerograms are thought to be due to hysteresis in the sensor, problems in the analog-to-digital converter, and tilting or rotation of the ground [Boore *et al.*, 1980; Boore *et al.*, 2002; Trifunac and Todorovska, 2001]. Problems often occur due to changes in the base level of the acceleration record during or after violent shaking. Analysis of these errors may be complicated by recordings that begin after the first P-wave arrival or which stop before shaking has stopped. These small offsets in the reference level of motion create large errors in the integrated record [Boore *et al.*, 2002]. In addition, very small angles of ground tilt may lead to shifts in the baseline in both horizontal acceleration components. This may be due to actual tectonic tilt of a large scale area, or to more localized ground failure during an earthquake [Clinton, 2004; Trifunac and Todorovska, 2001]. If there are non-negligible offsets in the vertical direction, then the offsets may not be easily ascribed to tilt at all, and may be related to nonlinearities within the seismometer itself [Clinton, 2004; Trifunac and Todorovska, 2001].

This study investigates the characteristics of the acceleration errors and the evaluation of methods to correct them, given that independent measurements of displacement are now available from 1 Hz GPS observations. We review the current methods for processing strong motion signals, compare 1 Hz GPS and seismic data, discuss the nature of some of the errors in the seismic acceleration records, and introduce techniques to combine 1 Hz GPS and seismic data to retrieve more accurate near source displacements.

Strong motion data processing

Historically, reliable estimates of the peak ground acceleration and the acceleration response spectra have been the primary products of strong motion monitoring. With advances in digital sensor technology, however, (digital, higher dynamic range sensors with longer pre-event and post event buffers), there is great interest in extending the usable frequency band to lower frequencies. In the typical uses of the data, the frequencies of interest are around 1 Hz, and the objective of strong motion data processing is to estimate those products from the usable frequency band of the record and filter out low frequency noise [Shakal *et al.*, 2004]. The noise spectrum increases linearly as period increases, so criteria have been defined for the low frequency cutoff, such as where the signal to noise drops below a factor of 2-3 [Trifunac, 1977; Trifunac and Lee, 1978]. Similar processing systems are in use at the California Strong Motion Instrument

Program (CSMIP) [Shakal et al., 2005], the National Strong Motion Program (NSMP) [Converse and Brady, 1992; Stephens and Boore, 2004], and the Pacific Earthquake Engineering Research Center (PEER) [Abrahamson and Silva, 1997; Darragh et al., 2004] in the United States, and the Taiwan Strong Motion Instrumentation Program (TSMIP) array [Loh, 2004].

The basic method, as implemented in NSMP processing [Converse and Brady, 1992], uses high pass (0.02 Hz) and low pass (50Hz) Butterworth filters. After removing the mean, tapering, and removing the instrument response, the filter corner frequencies are adjusted by reviewing the initial estimates of the spectra. The velocity and displacement are computed by time domain integration. Then the acceleration, velocity, and displacement are plotted and reviewed visually.

Techniques for correcting acceleration baseline errors to retrieve lower frequency information and static offsets typically fit a slope to the velocity trace and then subtract the derivative of this correction signal from the original accelerometer record before a final integration to velocity or displacement [Boore, 2001; Boore et al., 2002]. With this method, a displacement record is recovered that is constant after strong ground shaking has ended, though it is a very subjective process. It has been suggested that while a zero post-event velocity is a condition for a baseline-corrected signal, it may not be well enough constrained to recover an accurate coseismic displacement [Boore and Bommer, 2005]. In the absence of GPS data, stability of the correction technique and general agreement in final offsets among nearby sites are criteria that are used to judge the reliability of the baseline corrections.

The procedure of baseline correction to preserve static permanent or tectonic displacements in near-source recordings (< 20 km from the fault), as implemented in the PEER database processing is as follows:

- 1) Make a least squares fit to the integrated acceleration (velocity records) using three functional forms: linear fit to velocity, bilinear piecewise continuous fit, and a quadratic fit to velocity.
- 2) Make a systematic search of the start time of the fitting function to determine the best fitting functional form.
- 3) Differentiate the best fitting function and then remove it from the original acceleration trace.
- 4) Low pass filter with a causal Butterworth 4 pole filter with corner near 50Hz to remove high frequency noise.
- 5) Time integrate acceleration trace to produce velocity and displacement time histories.
- 6) Plot acceleration, velocity, and displacement and review visually.

A detailed review of this technique to retrieve absolute displacements applied to the 1999 Hector Mines earthquake and the 1999 Chi-Chi, Taiwan, earthquake demonstrates results that appear to be consistent with the previously mentioned criteria – zero post-event velocity and constant static displacement, stability in the correction algorithm and final

offset consistency among nearby sites [Boore, 2001; Boore et al., 2002]. However, there are no independent means for verifying the final displacements. Total displacement results from both earthquakes have been compared to static displacements retrieved from static GPS measurements processed for a daily average position. These presume that the entire static displacement occurred during the earthquake with no postseismic deformation during the averaging period following the event. The seismic displacement time series derived from the acceleration cannot be verified during and immediately following the shaking with the static GPS result alone. In the sections that follow, we apply the strong ground motion processing procedure described above compare the results to the GPS displacement time series to formally estimate the uncertainties involved with retrieving absolute displacement.

1 Hz GPS measurements

The Global Positioning System is a constellation of satellites used to determine meter-level positions in real-time. It is primarily used for navigation. The geodetic community has also developed methods for mm-level positioning in non-real-time [Segall and Davis, 1997]. In order to achieve this precision, geodetic software must accurately model the orbital parameters of the satellites, account for atmospheric delays, and solve for clock drifts and cycle ambiguities. Generally geodetic users estimate positions over long periods, ~ 24 hours. This allows static displacements of a site due to an earthquake to be computed, where an entire day or multiple days of GPS data are processed to retrieve a single average position before the earthquake and a single average position after the earthquake.

For 1-Hz GPS applications [Larson et al., 2003], positions are estimated every second rather than averaged. In this study, positions are estimated using the GIPSY software [Lichten and Border, 1987] with orbits held fixed to precise IGS values [Beutler et al., 1994]. Positions are defined in the ITRF2000 reference frame [Altamimi et al., 2002]. Reference sites were chosen to be more than 400 km from the source region to avoid any contamination by strong ground motion at the reference sites, as was seen in [Irwan et al., 2004]. The method is described in more detail in the electronic supplements for [Larson et al., 2003] and [Miyazaki et al., 2004a]. Thirty second sampling GPS records are also analyzed.

Datasets

Four datasets are available for this investigation: the 2004 Mw 6.0 Parkfield, CA, earthquake, the 2003 Mw 6.5 San Simeon, CA, earthquake, the 2002 Mw 7.9 Denali, AK, earthquake, and the 2003 Mw 8.0 Tokachi-Oki earthquake. Examples of GPS time series are shown below for each event.

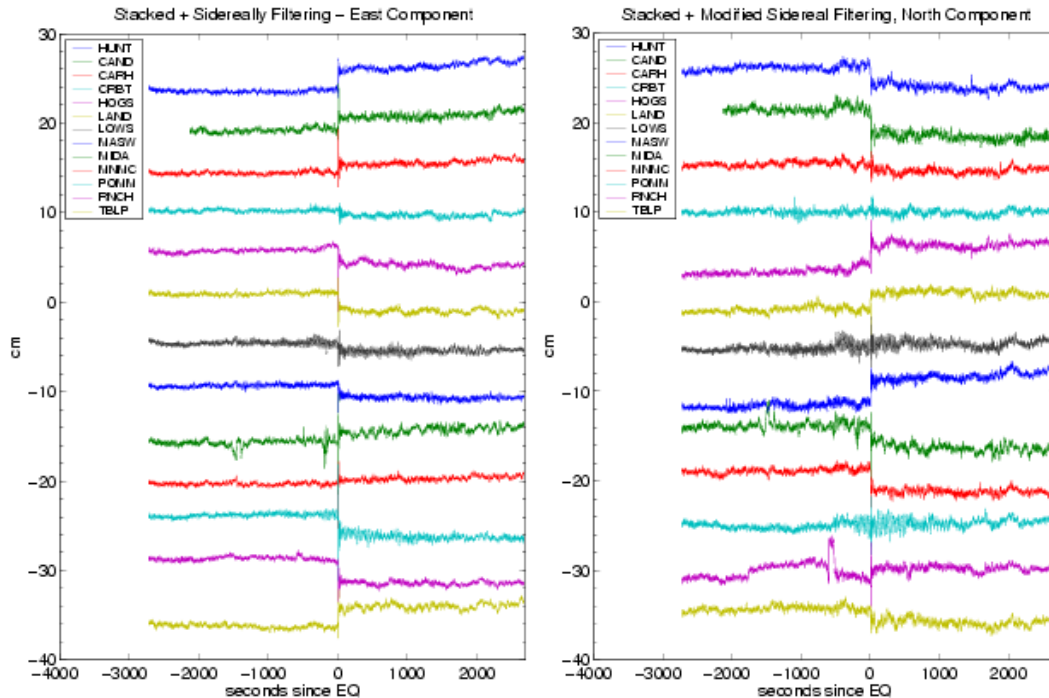


Figure 1 1 Hz GPS solutions for 13 sites near Parkfield for approximately 45 minutes before and after the earthquake. The earthquake occurred at time 0 and produces a step offset in the traces. Traces such as HUNT and MIDA show clear trends in the signal associated with postseismic deformation and do not return to a static level in the time directly following the earthquake (figure provided by Kristine Larson, personal communication).

We show a comparison between two GPS sites and collocated strong motion sensors from the Parkfield strong motion array [Shakal et al, 2005] (data from the CISN Engineering Data Center at [Http://www.cisn-edc.org](http://www.cisn-edc.org)) in Figure 3. The strong motion data has already been integrated in the volume 2 product, presumably following the processing systems in use by the California Strong Motion Instrument Program (CSMIP) [Shakal et al, 2004]. It is clear that GPS data is at the limit of the sampling interval needed to retrieve useful information, however the GPS data shows a clear difference in preseismic and postseismic level that is filtered out of the seismic data.

Example records from the San Simeon earthquake are shown in Figure 4. The lower frequency energy evident in the waveforms from the San Simeon earthquake compared to the Parkfield earthquake clearly illustrate that the sample rate of the 1 Hz GPS is sufficient to constrain the ground motion, which was not as clear for the Parkfield earthquake. Examples from the Denali earthquake are shown in Figure 5 and the Tokachi-Oki earthquake in Figure 6.

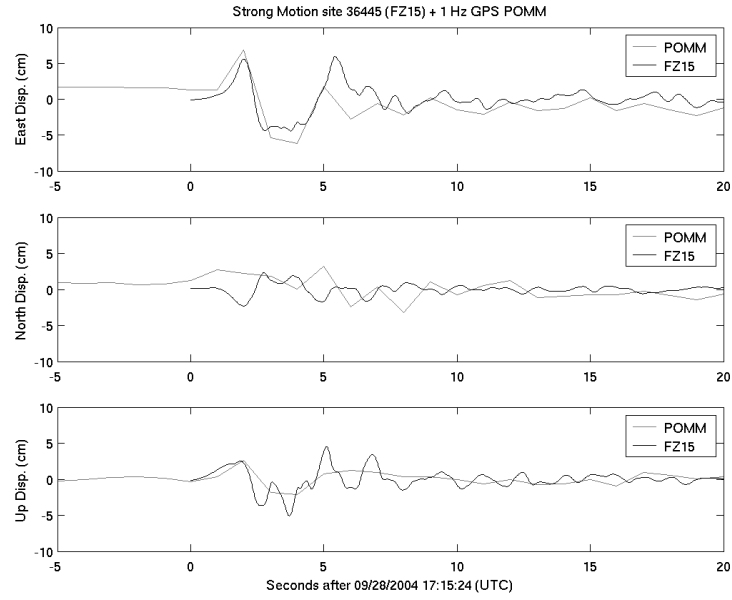


Figure 2 Comparison of 1 Hz GPS from POMM with strong motion recordings from FZ15.

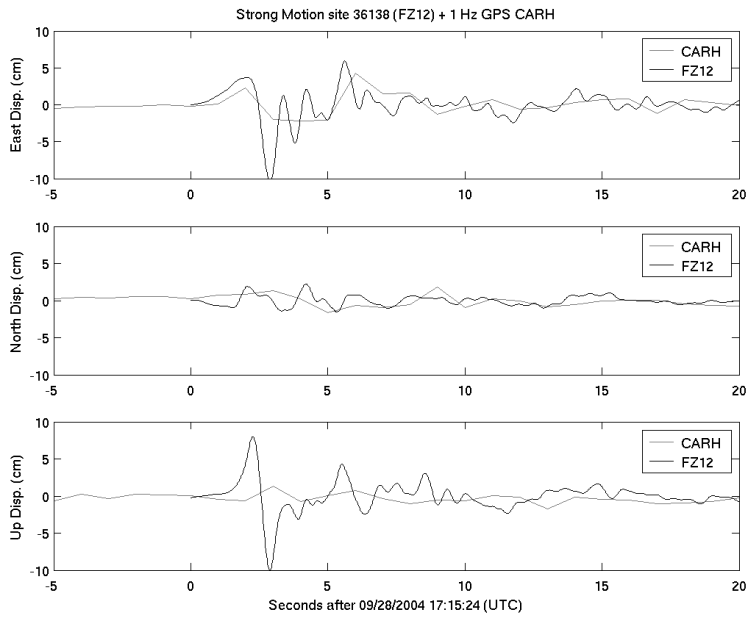


Figure 3 Comparison of 1 Hz GPS from CARH with strong motion site FZ12.

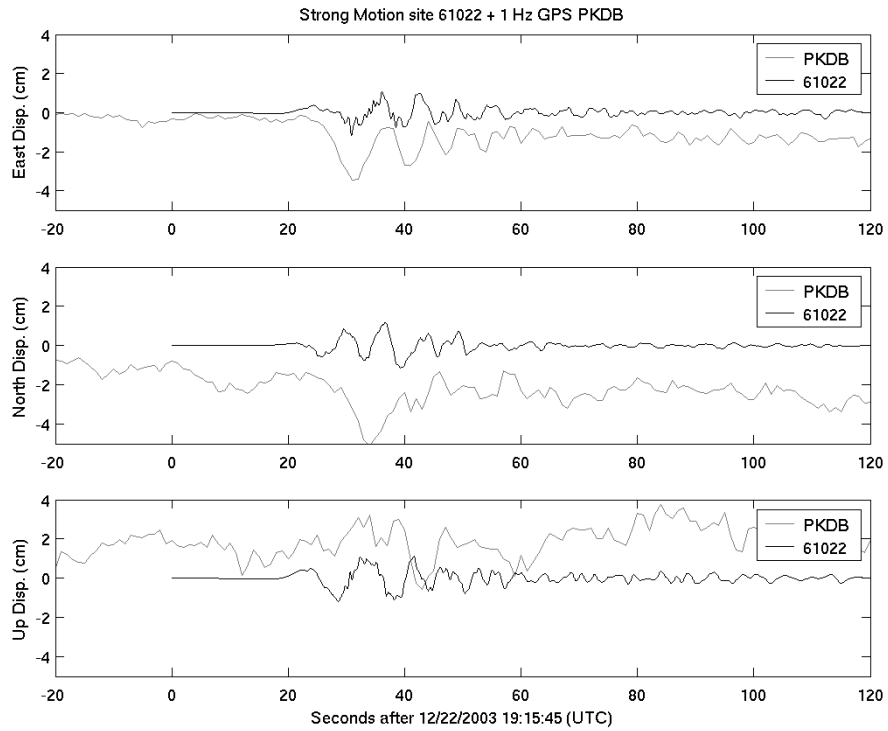


Figure 4 Collocated records from the San Simeon earthquake from the 1 Hz GPS site and strong motion instrument in Parkfield (PKDB). The version 2 strong motion data has been filtered so does not preserve any static displacement. The original uncorrected records will be used in our processing.

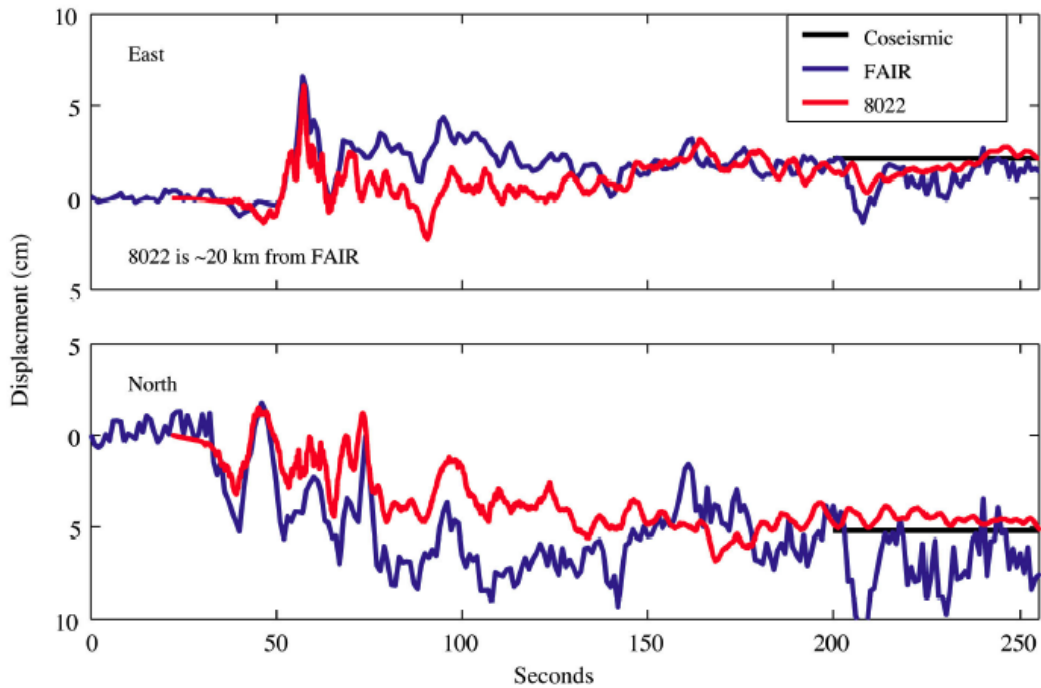


Figure 5 Nearly collocated recordings from the Denali earthquake. The GPS time series has been shifted by 3 seconds to account for the offset in distance (figure from Larson et al., 2003).

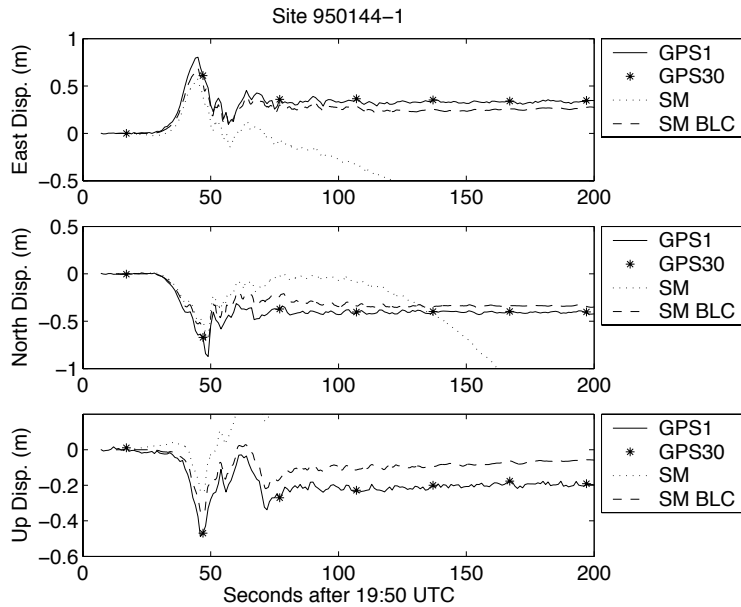


Figure 6 Example of 1 Hz GPS displacement from the Tokachi-Oki earthquake for site 950144 (solid line), GPS 30 second solution for displacement (stars), uncorrected integrated strong motion for Knet site HKD110 (dotted line) and baseline corrected integrated integrated strong motion record (dashed line).

For these datasets, short-term precision has been evaluated as 4, 7, and 15 mm for the east, north, and vertical components [Miyazaki *et al.*, 2004a].

Method for Combining GPS and seismic data to retrieve optimal near source displacements

The following method was developed to combine the 1Hz GPS solution and the seismic data to constrain the long period instability during integration of accelerometer records and correct for any unpredictable offsets present within them that may be approximated as step functions. An inverse problem is constructed to solve for both the ground displacements at the seismic sensor, as well as a record of any offsets (noise) in the acceleration record. A discrete acceleration time history can be related to displacements via a central difference differentiation operator of the form:

$$\frac{1}{dt^2} \begin{bmatrix} 1 & -2 & 1 & \cdots & 0 & 0 & 0 \\ 0 & 1 & -2 & \cdots & 0 & 0 & 0 \\ \vdots & \vdots & \vdots & \ddots & \vdots & \vdots & \vdots \\ 0 & 0 & 0 & \cdots & -2 & 1 & 0 \\ 0 & 0 & 0 & \cdots & 1 & -2 & 1 \end{bmatrix} \begin{bmatrix} u_1 \\ u_2 \\ u_3 \\ \vdots \\ u_{n-2} \\ u_{n-1} \\ u_n \end{bmatrix} = \begin{bmatrix} a_2 \\ a_3 \\ \vdots \\ a_{n-2} \\ a_{n-1} \end{bmatrix}$$

$$\equiv [D^2][\bar{u}_{ground}] = [\bar{a}_{ground}]$$

where u_i is a displacement time series at time i , a_i is the corresponding acceleration time series, and dt is the sample interval of the two discrete signals. Additional constraints are added using collocated GPS measurements. The inverse problem is of the form

$$\text{forward: } \bar{A}\bar{u}_{ground} = \bar{d}$$

$$[A][\bar{u}_{ground}] = \begin{bmatrix} \bar{a}_{SM} \\ \bar{u}_{GPS} \end{bmatrix}$$

$$\text{inverse: } \bar{u}_{ground} = A_g^{-1}\bar{d}$$

where d represents the data vector, containing both the strong motion acceleration time series and any available collocated GPS displacement time series. The matrix A is the operator for the system, containing both differentiators and identity matrices. u_{ground} is the unknown vector of actual ground displacements. A_g^{-1} is the generalized inverse of A including the covariance matrix. The unknown accelerometer offsets, $n_{noiseparameters}$ are introduced as a series of step functions that can occur at any time during the time series. This modifies the inverse problem to be

$$\begin{bmatrix} \bar{a}_{SM}^{10Hz} \\ \bar{u}_{GPS}^{1Hz} \\ \bar{u}_{GPS}^{30s} \end{bmatrix} = \begin{bmatrix} [D^2] & [H] \\ [I^{10Hz \rightarrow 1Hz}] & [0] \\ [I^{10Hz \rightarrow 30s}] & [0] \end{bmatrix} \begin{bmatrix} \bar{u}_{ground}^{10Hz} \\ \bar{n}_{noiseparameters} \end{bmatrix}$$

$$A_g^{-1} = [A^T C_d^{-1} A]^{-1} A^T C_d^{-1}$$

$$[C_d^{-1}] = \begin{bmatrix} \left[\frac{1}{\sigma_{SM}^2} \right] & [0] & [0] \\ [0] & \left[\frac{1}{\sigma_{1HzGPS}^2} \right] & [0] \\ [0] & [0] & \left[\frac{1}{\sigma_{30sGPS}^2} \right] \end{bmatrix}$$

in which D^2 is the central difference operator, I is a reduced identity matrix that selectively samples the displacement vector at 1s or 30s to correspond with the GPS sampling, operator H contains the Heaviside functions that map step function offsets at fixed times, and C_d^{-1} is a weighting matrix, based on the uncertainties in the data. Estimates for the uncertainties in the GPS data processing lead to a value of 4 mm for the east component GPS record, 7 mm for the north component and 15 mm for the vertical component [Miyazaki *et al.*, 2004a]. The goal is to fit the data such that the agreement between the GPS and strong motion is within the threshold value. The seismic data are weighted by the digitization precision of the instruments, which weights the seismic data more heavily than the GPS data as justified by the higher precision, to maintain the higher frequency character of the desired signal. Because 1 Hz GPS data are not always available, we have also tested the method for constraining portions of the seismic signal using 30 second GPS data.

In the first phase of processing, the accelerometer data are decimated from to produce a 10 Hz time series. The point of combining the strong motion data with the GPS data is to retain the higher frequency character of the accelerometer data while gaining the low frequency displacement behavior of the GPS data. Frequencies above 10 Hz, being outside the frequency range of interest, are removed to reduce the time and memory requirements for the least-squares procedures. A standard integrated strong motion displacement signal may be seen in Figure 6, compared to the nearby GPS station. Notice the severe effect of extremely small acceleration shifts when the signal is integrated, producing a parabolic trend in displacement and a slope in velocity.

The next phase is to correct for possible unknown mis-orientation of the sensors. As noted previously in [Clinton, 2004; Miyazaki *et al.*, 2004a], a misalignment of the seismometer could very easily produce significant differences between the seismic and GPS records. Both the strong motion acceleration and GPS displacement signals were high pass filtered at 30 s period to remove static offsets. A grid search approach was used to compare high-pass filtered GPS signals with their high-pass filtered strong-motion counterparts over a range of possible rotation angles. The minimum in an error function quantifying the difference is used to determine the rotation angle. The standard deviation of the difference between the GPS and integrated strong motion signals normalized by the maximum amplitude of the filtered GPS signal is used as an error measure for the agreement between these filtered signals.

$$Err = \frac{\sum_{j=1}^2 \sum_{i=1}^{nt} (u_{SMi,j} - u_{GPSi,j})}{(2 \cdot nt - 1) \cdot \max(u_{GPSi,j})} \quad (3)$$

in which $u_{SMi,j}$ are the filtered doubly integrated strong motion time series (decimated to 10 Hz) for component j , $u_{GPSi,j}$ are the filtered zero mean 1 Hz GPS displacements (resampled at 10 Hz) for component j , and nt is the number of time samples.

For comparison purposes, the strong motion signal is baseline corrected using a procedure similar to the methodology employed for the PEER database [Boore, 2001].

The baseline correction removes the trend present in the velocity trace. The baseline corrected seismograms show good agreement with GPS results early in the event history (Figure 6). The correction removes the obvious parabolic baseline error for the N-S component and produces a time series where the velocity is zero and displacement is constant after the shaking has stopped. Unfortunately, due to the nature of integration, very small deviations in the velocity signal from a linear baseline can produce a large discrepancy in the displacement record. The acceleration record in this particular case is reasonably well behaved, but still produces some erroneous offsets of as much as 20 cm. These signals are calculated for comparison only and are not used further in the constrained integration scheme.

Finally, the actual combined displacement solution is calculated as described in the inverse problem above, using the unfiltered accelerometer records, using a simple step function model to represent the unknown acceleration offsets, and utilizing 1 second and 30 second GPS data to constrain the signal. While it might be expected that a step function offset that was due to an instantaneous tilt of the 3 component sensor would produce significant offsets on the two horizontal components at the same time, each component was computed separately. In this way the hypothesis of local ground tilt as the cause of offsets could be tested. Since the timing of the Heaviside step functions is unknown, an iterative search method is used where the starting time of the step function is assumed and the inverse problem is solved. The start time of the step is changed and the process repeated. The minimum misfit solution is selected. If a single step function does not satisfy the misfit criterion of 0.09, then a second step function is added and the iterative process is repeated for the second step function. If the two step function solution has a misfit less than 0.09 or has a misfit reduction of more than 50% over the single step function solution, then it is kept as the optimal solution. Otherwise the single step function solution is retained. An example showing the result of the constrained inversion is given in Figure 7. The combined displacement removes the estimation noise of the GPS data and replaces it with a more precise integrated displacement at that frequency. The combined displacement is smoother than the 1Hz GPS, but has a reliable coseismic offset.

There is a possibility that the ground motion contains a significant component of time varying tilt [Graizer, 2004]. To explore this possibility, we perform a test where we specify in advance the starting time of a large number of step functions (10, for example) and solve the inverse problem. With a generalized inverse and weak constraint on the size of the step functions, this ill-constrained problem can be solved. We found that this approach usually produces one or two large steps with a large number of small steps that are very poorly constrained, lending support to the approach of limiting the number of steps. The solutions with one or two steps then can be considered a test of the hypothesis that the data can be satisfied using this simple model. Data sets that fail to retrieve a satisfactory solution indicate the possible presence of time-varying tilt.

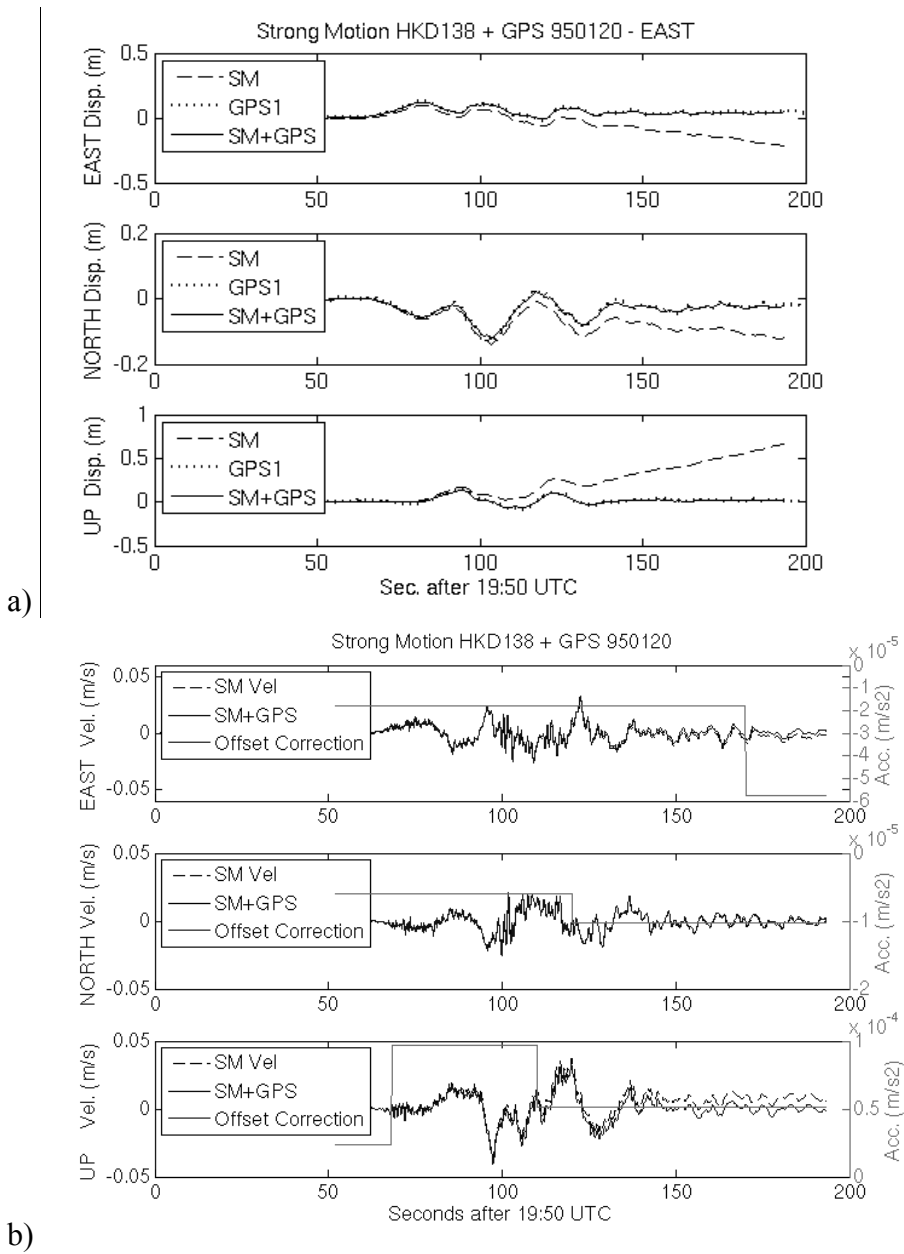


Figure 7 (a) Displacement constrained by a combination of GPS and strong motion data is shown for GPS site 950120 and seismic site HKD138 (solid line, SM+GPS). The integrated uncorrected strong motion data (dashed, SM) have large errors. (b) velocity seismograms for the same site pairs.

Figure 8 shows an example of the final solution for the combined GPS and seismic displacement time series for several sites. Superimposed are the step function acceleration offset solutions for each component. A few features are particularly noticeable. First of all, it is clear that the step function model for long period offsets appears to be valid for most cases, since the resulting high frequency displacements match quite closely the 1 Hz GPS. In the sites examined, one or two steps were sufficient for the noise model. In addition, the step functions appear to arise simultaneously on

more than one component. The step functions were usually found to occur well after the peak acceleration.

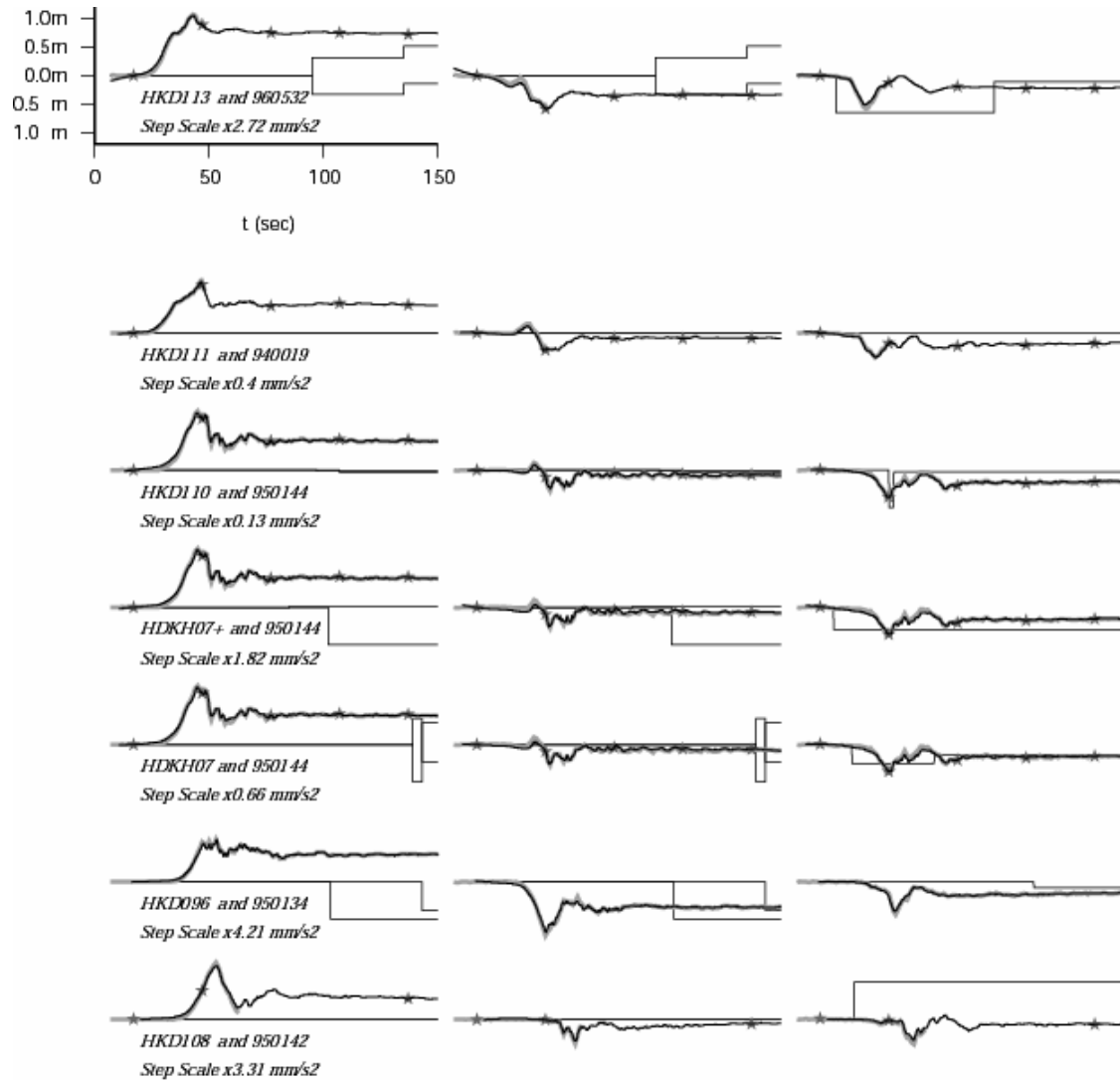


Figure 8a Examples of constrained displacement seismograms (dark line, SM+GPS) for several sites for the same event, from 0 km to 155 km from the hypocenter, in order of increasing distance. 1Hz GPS (gray line) and 30s GPS (stars) are also shown. Displacement is in meters using the same scale for all seismograms on the panel. The timing of the step function offsets is shown with the thin black lines, scaled by the amount indicated by the text in mm/s^2 . Components are East, North, and Up. Both horizontal step function components have been plotted with the East and North components to clarify the relative timing of the rotated components.

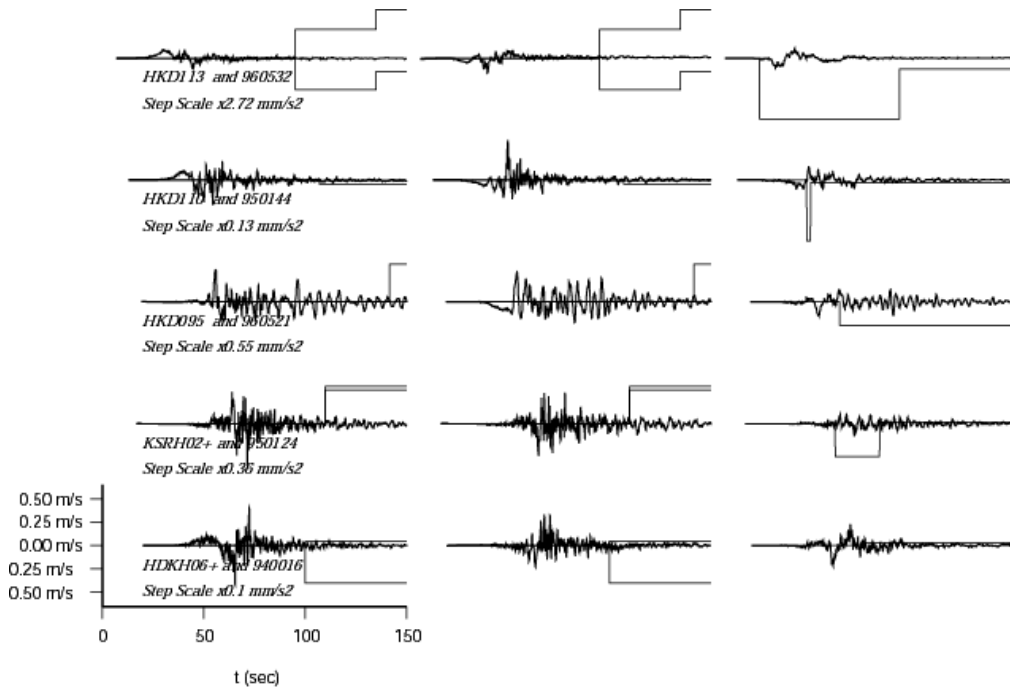


Figure 9 Constrained velocity seismograms for several sites at distances 0 km to 155 km from the hypocenter. Velocity is in meters per second using the same scale for all seismograms on the panel. The timing of the step function offsets is shown with the thin black lines, scaled by the amount indicated by the text in mm/s^2 . Components are local sensor East, North, and Up.

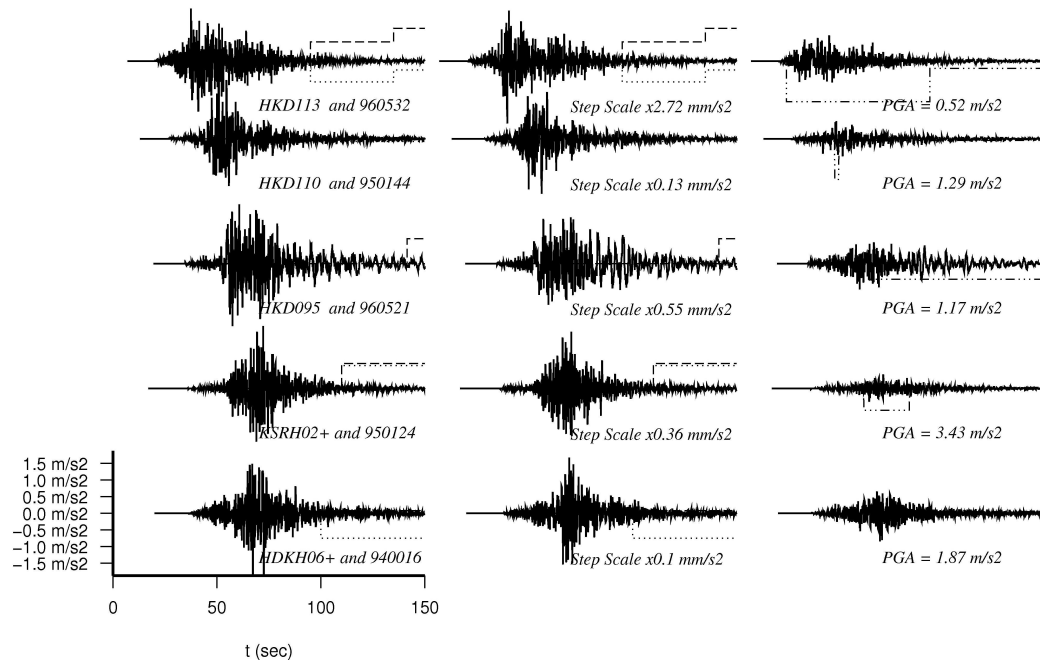


Figure 10 Constrained acceleration records for several sites at distances of 0 to 155 km from the hypocenter. Acceleration is in m/s^2 . The timing of the step function offsets is shown with the thin black lines, scaled by the amount indicated by the text in mm/s^2 . Components are East, North, and Up. Records for each site are normalized to the peak ground acceleration. T

Comparison of constrained solution to alternative approaches

In all cases, the baseline-corrected displacement signal that was calculated without GPS as a constraint produced a time series with a post-event constant displacement. In some cases, the BLC coseismic displacement matched the GPS within the GPS margin for error. However, there was no reliable relationship that could be used to predict which sites might recover a correct versus an incorrect baseline corrected coseismic displacement. This is because although a flat post-event displacement response is a necessary criterion for a baseline correction scheme, it may not reflect the true displacement [Boore and Bommer, 2005]. Part of the problem with the baseline correction scheme is the lack of knowledge of the presence and number of step function offsets. When there can be more than one possible step within the active portion of the signal it becomes a nontrivial task to decide how many steps there should be and when they should take place, not to mention what their magnitude should be. There is a tendency for the differences between the 1 Hz GPS and the unconstrained baseline corrected strong-motion coseismic displacements to be larger at sites that are closer to the earthquake focus. A challenge with a traditional baseline correction scheme is the need for a well-defined pretrigger signal to establish an initial baseline. The GPS constrained solution has no such requirement, and it is possible to retrieve useful displacement signals when the initial P-wave was not captured by the accelerometers. For the BLC signals, the magnitude of the resulting static displacement is highly sensitive to the precise timing of the offset. If the coseismic offset is in disagreement with the GPS, the timing of the baseline correction offsets are likely to be in error. Therefore we hesitate to draw further conclusions from these baseline correction errors.

For comparative purposes, an error estimate for each component of the retrieved optimal displacements can be computed that is consistent with the normalized standard deviation error used previously in the examination of site orientations. In this case, instead of using the difference between filtered displacement signals, the residual between the constrained solution and the unconstrained, rotated strong motion signal modified by the noise model solution is used. This is described as

$$Err = \frac{\sum_{i=1}^{nt} \left(\int_0^{t_i} \int_0^{t_i} (a_{SM} - a_{step}) dt^2 \right) - u_{GPSi}}{(nt - 1) \cdot \max(u_{GPSi})} \quad (9)$$

in which a_{SM} are the unfiltered rotated strong motion accelerations, a_{step} is the solved step function noise model, and $u_{GPSi,j}$ are the 1 Hz GPS displacements (resampled at 10 Hz) for component j , and nt is the number of time samples. Once again, the strong motion time series was shifted in time by an amount proportional to the difference in epicentral distance.

There is an additional point of note. We tested the possibility that 30 s data could be used as the constraint, rather than the 1 Hz data. As Figure 11 shows, the results from the use of a 30 second constraint alone compare well to the fully constrained solution. This would be of most benefit for large events where there are a few 30 s samples within the major period of strong ground motion, and where the coseismic offsets are greater than the error level of the GPS estimates. However, 30 s GPS data are not sufficient for resolving misorientations of the sensors.

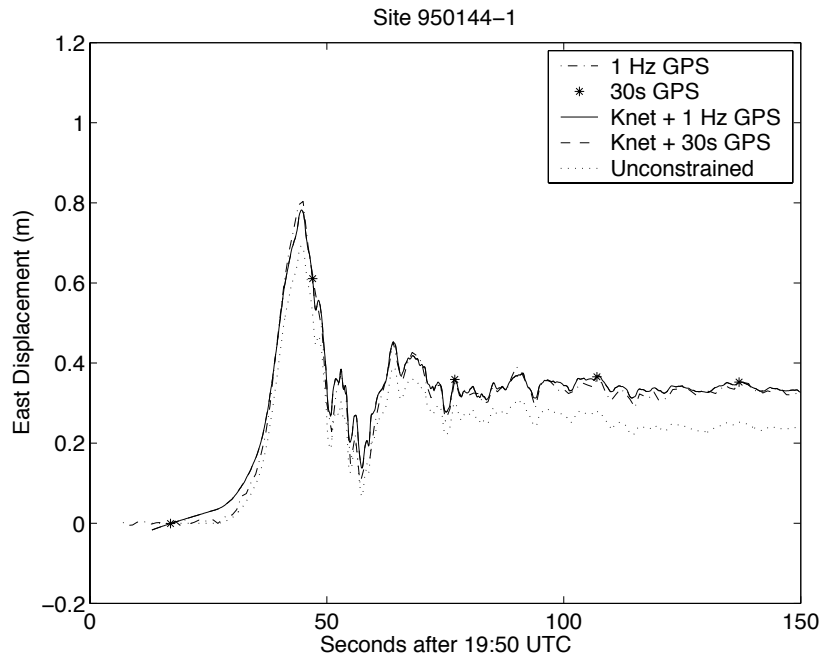


Figure 11 Constrained displacement solutions for 950144 and HKD110 using the full 1 Hz GPS constraint (solid line, seismic +1Hz GPS), and 30 second GPS constraint only (dashed line, seismic + 30s GPS). The original 1 Hz GPS time series is shown as a dot-dashed line, and the 30s GPS is shown by stars. The solution using only the 30s GPS as a constraint is virtually identical to the result using the 1Hz GPS for an event of this magnitude. Some differences are evident in the early part of the record, which may be due to the relatively short pre-trigger time series. A baseline corrected strong motion signal is also shown for comparison, as a dotted line.

Conclusions

Traditional techniques for recovering a coseismic static offset by making a baseline correction to velocity seismograms to account for one or two step functions in acceleration were found to be adequate for only a small number of cases. The comparison of integrated strong motion records with 1 Hz GPS displacement records indicates that only 5% of the time does the static displacement retrieved from baseline correction processing agree with the actual displacement to within 9%. This quantity 9% is approximately the assumed accuracy of the ground motions used in source inversions [e.g. Miyazaki *et al.*, 2004].

We have developed a constrained inversion technique, such that the optimal displacement records were found that satisfy the 1 Hz GPS data and the seismic data while simultaneously solving for a single step function offset, or maximum two step offsets, in the acceleration record. The acceptable level of misfit is determined by comparing the high pass filtered signals. Potential explanations for the offsets could be the tilt of the sensor, electronic noise, or mis-orientation of the sensor.

We have demonstrated the potential for using these techniques for colocated strong motion and 30 second GPS sites. Results using 1 Hz and 30 second GPS time series were compared and showed very good agreement. For an event the size of the Hokkaido event, where there is significant energy at frequencies of 20 sec and lower, the integration of the seismic waveforms is sufficiently constrained by the 30 s GPS solutions. This extends the applicability for using the technique to many more sites where 30 s GPS data are available. This 30 s data, however, would not be sufficient for checking the sensor orientation.

Often, for source inversion studies, seismic data are used in conjunction with coseismic offsets determined from daily GPS solutions, essentially an average position for the GPS site using data recorded continuously over one day before compared to the solution for one day after. This assumes that there was no change in site position over the daylong period. Using 1 Hz GPS allows one to distinguish better between coseismic and postseismic displacement, which can be important because of the potential for large postseismic changes within the first 24 hours after the event, as was the case for the Hokkaido earthquake [Miyazaki *et al*, 2004b].

Bibliography

- Emore, G.L., Haase, J.S., Choi, K., Larson, K.A. and Yamagiwa, A., 2007. Recovering seismic displacements through combined use of 1-Hz GPS and strong-motion accelerometers. *Bulletin of the Seismological Society of America*, 97(2): 357-378.
- Larson, K., Miyazaki, S., Choi, K., Hikima, K., Koketsu, K., Haase, J., Emore, G. and Yamagiwa, A., 2006. Modeling the rupture process of large earthquakes using 1-Hz GPS, *Seismological Society of America Annual Meeting, San Francisco, CA*, pp. 190.
- Emore, G., Haase, J.S., Choi, K., Larson, K.M. and Yamagiwa, A., 2005. Recovering Absolute Seismic Displacements Through Combined Use of 1 Hz GPS and Strong Motion Accelerometers, *American Geophysical Union Fall Meeting. EOS Trans. AGU, San Francisco*, pp. Abstract S21B-0215.

References

- Abrahamson, N. A., and W. Silva (1997), Empirical response spectral attenuation relations for shallow crustal earthquakes, *Seis. Res. Lett.*, **68**, 94-127.
- Altamimi, Z., P. Sillard, and C. Boucher (2002), ITRF2000: A new release of the International Terrestrial Reference Frame for Earth science applications, *J. Geophys. Res.*, **107**, 2214.

- Aoi, S., K. Obara, S. Hori, K. Kasahara, and Y. Okada (2000), New strong-motion observation network: Kik-net, *Eos Trans. AGU*, **81**(48), Fall Meet. Suppl., Abstract S71A-05
- Aoi, S., T. Kunugi, and H. Fujiwara (2004), Strong motion seismograph network operated by NIED: K-net and KiK-net, *Journal of Japan Association for Earthquake Engineering*, **4**, 65-74.
- Beutler, G., I. Mueller, and R. Neilan, (1994), The International GPS Service for Geodynamics (IGS): development and start of official service on January 1, 1994, *Bull. Geod.*, **68**, 39-70.
- Boore, D. M., and J. J. Bommer, (2005), Processing of Strong-motion accelerograms: needs, options, and consequences, *Soil Dynamics and Earthquake Engineering*, **25**, 93-115.
- Boore, D. M., Stephens, C. D., and Joyner, W.B. (2002), Comments on baseline correction of digital strong-motion data: Examples from the 1999 Hector Mine, California, earthquake, *Bull. Seismol. Soc. Amer.*, **92**, 1543-1560.
- Boore, D. (2001), Effect of baseline corrections on displacements response spectra for several recordings of the 1999 Chi-Chi, Taiwan, earthquake, *Bull. Seism. Soc. Am.*, **91**, 1199-1211.
- Boore, D. M., et al. (1980), Peak Acceleration, Velocity, and Displacement from Strong-Motion Records, *Bull. Seismol. Soc. Amer.*, **70**, 305-321.
- Castellani, A., and Z. Zembaty (1994), Stochastic modeling of seismic surface rotations, *Natural Hazards*, **10**, 181-191.
- Celebi, M. (2000), GPS in dynamic monitoring of long-period structures, *Soil Dynamics and Earthquake Engineering*, **20**, 477-483.
- Clinton, J. F. (2004), Modern Digital Seismology - Instrumentation, and Small Amplitude Studies in the Engineering World, PhD Thesis, California Institute of Technology.
- Clinton, J. F. (2006), personal communication.
- Converse, A. M., and A. G. Brady (1992), BAP: Basic Strong-Motion Accelerogram Processing Software; Version 1.0. US Geological Survey Open File Report 92-296A, Open File Report, 178 pp, United State Geological Survey, Menlo Park, CA.
- Darragh, B., W. Silva, N. Gregor (2004), Strong motion record processing for the PEER Center, paper presented at Invited Workshop on Strong-motion Record Processing convened by the Consortium of Organizations for Strong-Motion Observation Systems (COSMOS), 26-27 May 2004, COSMOS, Richmond, CA, 26-27 May 2004.
- Graizer, V. M. (2004), Record Processing considerations for the effects of tilting and transients, Proc. Invitational Workshop on Strong Motion Record Processing, May 26-27, 2004, COSMOS, Richmond CA.
- Hartzell, S. H., and T. H. Heaton (1983), Inversion of Strong Ground Motion and Teleseismic Waveform Data for the Fault Rupture History of the 1979 Imperial-Valley, California, Earthquake, *Bull. Seismol. Soc. Amer.*, **73**, 1553-1583.
- Honda, R., S. Aoi, N. Morikawa, H. Sekiguchi, T. Knugi, and H. Fujiwara (2004), Ground motion and rupture process of the 2003 Tokachi-oki earthquake obtained from strong motion data of K-net and KiK-net, *Earth Planets And Space*, **56**, 317-322.

- Igel, H., U. Schreiber, A. Flaws, B. Schuberth, A. Velikoseltsev, and A. Cochard (2005), Rotational motions induced by the M8.1 Tokachi-oki earthquake, Sept 25, 2003, *Geophysical Research Letters*, **32**.
- Irikura, K. (2006), personal communication.
- Irwan, W. D., Moser, M. A., Peng, C-Y (1985), Some observations on strong-motion earthquake measurement using a digital acelerograph, *Bull. Seismol. Soc. Am.*, **75**, 1225-1246.
- Irwan, M., F. Kimata, K. Hirahara, T. Sagiya, and A. Yamagiwa (2004), Measuring ground deformations with 1-Hz GPS data: the 2003 Tokachi-oki earthquake (preliminary report), *Earth Planets Space*, **56**, 389-393.
- Ji, C., K.M. Larson, Y.Tan, K.W. Hudnut, and K. Choi (2004), Slip history of the 2003 San Simeon earthquake constrained by combining 1-Hz GPS, strong motion, and teleseismic data, *Geophysical Research Letters*, **31**.
- Kinoshita, S. (1998), Kyoshin net (k-net), *Seismol. Res. Lett.*, **69**, 309-332.
- Koketsu, K., K. Hikima, S. Miyazaki, S. Ide (2003), Joint inversion of Strong Motion and Geodetic Data for the Source Process of the 2003 Tokachi-oki, Hokkaido, Earthquake, *Earth Planets Space*, **55**, 1-6.
- Kramer (1996), *Geotechnical Earthquake Engineering*, 653 pp., Prentice Hall, Upper Saddle River, NJ.
- Larson, K. M., P. Bodin, and J. Gomberg (2003), Using 1-Hz GPS data to measure deformations caused by the Denali fault earthquake, *Science*, **300**, 1421-1424.
- Lichten, S. M., and J. S. Border, (1987), Strategies for high-precision global positioning system orbit determination, *Journal of Geophysical Research*, **92**, 12751-12762.
- Loh, C.-H. (2004), Strong motion data processing in Taiwan and its engineering application, paper presented at Invited Workshop on Strong-motion Record Processing convened by the Consortium of Organizations for Strong-Motion Observation Systems (COSMOS), 26-27 May 2004, COSMOS, Richmond, CA, 26-27 May 2004.
- Miura, S., Y. Suwa, A. Hasegawa, T. Nishimura (2004), The 2003 M8.0 Tokachi-Oki earthquake: How much has the great event paid back slip debts? *Geophys. Res. Lett.*, **31**.
- Miyazaki, S., K.M. Larson, K. Choi, K. Hikima, K. Kotetsu, P. Bodin, J. Haase, G. Emore, and A. Yamagiwa (2004a), Modeling the rupture process of the 2003 September 25 Tokachi-Oki (Hokkaido) earthquake using 1-Hz GPS data, *Geophysical Research Letters*, **31**.
- Miyazaki, S., P. Segall, J. Fukuda, and T. Kato (2004b), Space time distribution of afterslip following the 2003 Tokachi-oki earthquake: Implications for variations in fault zone frictional properties, *Geophysical Research Letters*, **31**.
- Miyazaki, S., T. Saito, M. Sasaki, S. Hatanaka, and Y. Iimura (1997), Expansion of GSI's Nationwide GPS Array, *Bull. Geographical Survey Institute*, **43**, 23-34.
- Okada, Y. (1985), Surface Deformation Due to Shear and Tensile Faults in a Half-Space, *Bull. Seismol. Soc. Amer.*, **75**, 1135-1154.
- Okada, Y., K. Kasahara, S. Hori, K. Obara, S. Sekiguchi, H. Fujiwara, and A. Yamamoto (2004), Recent progress of seismic observation networks in Japan - Hi-net, F-net, K-NET and KiK-net, *Earth Planets And Space*, **56**, XV-XXVIII.

- Segall, P. and J.L. Davis (1997), GPS applications for geodynamics and earthquake studies, *Annual Reviews of Earth and Planetary Science*, **25**,301-36.
- Shakal, A., V. Graizer, M. Huang, R. Borchardt, H. Haddadi, K. Lin, C. Stephens, and P. Roffers (2005), Preliminary analysis of strong-motion recordings from the 28 September 2004 Parkfield, California, Earthquake, *Seismol. Res. Lett.*, **76**, 27-39.
- Shakal, A. F., M. Huang, and V. Graizer (2004), CSMIP Strong-motion data processing, paper presented at Invited Workshop on Strong-motion Record Processing convened by the Consortium of Organizations for Strong-Motion Observation Systems (COSMOS), 26-27 May 2004, COSMOS, Richmond, CA, 26-27 May 2004.
- Spencer, B. F., E. Johnson, and J. Ramallo (2000), "Smart" isolation for seismic control, *Jsm International Journal Series C-Mechanical Systems Machine Elements and Manufacturing*, **43**, 704-711.
- Stephens, C. D., and D. M. Boore (2004), ANSS/NSMP Strong-motion record processing and procedures, paper presented at Invited Workshop on Strong-motion Record Processing convened by the Consortium of Organizations for Strong-Motion Observation Systems (COSMOS), 26-27 May 2004, COSMOS, Richmond, CA, 26-27 May 2004.
- Symans, M. D., G. J. Madden, and N. Wongprasert (1999), Semi-active hybrid isolation systems: addressing the limitations of passive isolation systems, *Proc. of Structures Congress*, ASCE, New Orleans, LA, April, 862-865.
- Trifunac, M. D. (1977), Uniformly Processed Strong Motion Earthquake Ground Accelerations in the Western United States of America for the Period from 1933 to 1971: Pseudo Relative Spectra and Processing Noise, Report CE 77-044, Univ. Southern California, Los Angeles, Los Angeles, CA.
- Trifunac, M. D., and V. Lee (1978), Uniformly Processed Strong Earthquake Ground Accelerations in the Western United States of America for the Period from 1933 to 1971: Corrected Acceleration, Velocity and Displacement Curves, Report CE 78-01, Dept. Civil Engineering, Univ. Southern California, Los Angeles, Los Angeles, CA.
- Trifunac, M. D., and M. I. Todorovska (2001), A note on the usable dynamic range of accelerographs recording translation, *Soil Dynamics and Earthquake Engineering*, **21**, 275-286.
- Wald, D. J., and T. H. Heaton (1994), Spatial and Temporal Distribution of Slip for the 1992 Landers, California, Earthquake, *Bull. Seismol. Soc. Amer.*, **84**, 668-691.
- Yagi, Y. (2004), Source rupture process of the 2003 Tokachi-oki earthquake determined by joint inversion of teleseismic body wave and strong ground motion data, *Earth Planets And Space*, **56**, 311-316.
- Yamagiwa, A., Y. Hatanaka, T. Yutsudo, and B. Miyahara (2006), Real time capability of GEONET system and its application to crust monitoring, *Bulletin of the Geographical Survey Institute*, **55**, 27.
- Yamanaka, Y., and M. Kikuchi (2003), Source process of the recurrent Tokachi-oki earthquake on September 26, 2003, inferred from teleseismic body waves, *Earth Planets And Space*, **55**, E21-E24.

